

Study of transient spark discharge properties using kinetic modeling

Lukáš Dvonč, Mário Janda

May 6, 2015

*Division of Environmental Physics, Faculty of Mathematics, Physics and Informatics,
Comenius University Bratislava,
Mlynská dolina F2, 84248 Bratislava, Slovakia*

Abstract

The kinetic model simulating plasma chemistry induced by Transient Spark (TS) discharge in air is presented in this work. The TS is a DC-driven self-pulsing discharge of streamer-to-spark transition type. Presented kinetic model defines the temporal evolution of reduced electric field strength E/N , gas temperature and density of neutrals N during the evolution of TS discharge, so that calculated electron density is in agreement with experimental results. We studied the mechanism of the streamer-to-spark transition and breakdown in the TS using this model. We assume that the breakdown mechanism in TS is based on the gas density decrease and can be summarized as follows: heating of the channel \rightarrow increase of the pressure \rightarrow hydrodynamic expansion \rightarrow decrease of N in the core of the channel \rightarrow increase of E/N \rightarrow acceleration of ionization processes. However, this mechanism is influenced by species accumulated due to previous TS pulses at higher TS repetition frequencies. Sensitivity analysis focused on major electron loss and production processes indicates an important role of the amount of O_2 dissociated by the previous pulses. Lower density of O_2 means lower rate of electron attachment, while accumulated atomic oxygen atoms lead to acceleration of electron detachment processes.

1 Introduction

Atmospheric pressure non-thermal plasma has a wide range of use in many industrial and environmental applications. In the recent years, non-thermal plasma based technologies were successfully implemented in processes such as surface modification, bio-decontamination, sterilization, plasma assisted combustion, or hazardous waste processing [1–8]. Further innovative applications are still being investigated.

Various electrical discharges can be used to generate reactive non-thermal plasmas. Among the most common are dielectric barrier discharge (DBD) [2], pulsed corona discharge [9] and streamer discharge [7]. However, there is no single universal type of discharge suitable for all applications. Thus, there is a constant demand for new atmospheric pressure discharges generating cold non-thermal plasma with high

electron density. For this reason we investigate an atmospheric pressure discharge named transient spark (TS).

The TS is a DC-driven self-pulsing discharge of streamer-to-spark transition type with the repetition frequency 1-10 kHz. During the spark phase of TS, the electron density as high as 10^{17} cm^{-3} can be achieved [10]. Generated plasma is thus strongly ionized for a short time. However, the TS spark current pulses are sufficiently short ($\sim 10\text{-}100 \text{ ns}$) to avoid thermalization of generated plasma. Unlike classical spark, the TS thus generates highly reactive non-equilibrium non-thermal plasma that was already successfully tested for several biological and environmental applications [11–14]. Basic research of TS using several electrical and optical diagnostic methods was also performed [10, 15–18]. However, further research of TS based on both experimental and computational techniques is needed for better understanding of chemical processes initiated by the TS.

The modeling of chemical kinetics aiming to calculate the density evolution of all species included in the kinetic model is an effective tool for complex systems description [9, 19]. In many cases, it is the most powerful way to solve problems where the complexity inhibits using analytical methods and direct experimental measurements. It is commonly used not only for modeling of cold plasma chemistry [20], but also for description of high temperature steady state arc plasma [21], nanosecond duration of streamer propagation [22], and other problems in plasma physics and chemistry.

The aim of this work is to present a chemical kinetic model developed for the TS discharge. This model can be used to determine the evolution of density of species, which are not measurable via available experimental techniques. Moreover, this model is able to describe macroscopic parameters such as plasma conductivity and current density in the plasma channel. The validity of the model was tested by comparing calculated electron densities with experimental data [10, 15].

2 Transient Spark

Figure 1 shows a schematic of the electric circuit used to generate the TS discharge. A positive polarity DC high voltage (HV) power supply connected to a metal needle HV electrode via a series resistor ($R = 5\text{-}10 \text{ M}\Omega$) is typically used to generate a positive TS discharge. The typical distance d between the tip of the HV electrode and a grounded planar electrode is 4-10 mm. More details can be found in [15, 16].

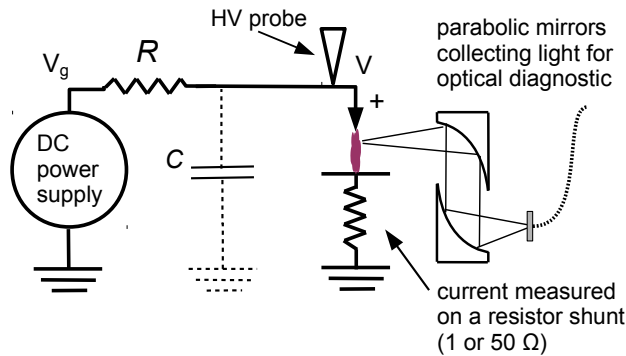


Figure 1: Schematic of the setup used to generate and diagnostic Transient Spark.

Transient spark is initiated by a streamer (phase A, upper chart in Fig. 2), when the potential on the stressed electrode reaches voltage V_{TS} , characteristic for the TS. This streamer creates a relatively conductive plasma bridge between the electrodes. This enables partial discharging of the internal capacitor C of the electric circuit generating TS, and heating of the gas inside this plasma channel. The gas temperature inside the plasma channel increases to ~ 1000 K (Fig. 3) during the streamer-to-spark transition phase (phase B, upper chart in Fig. 2), followed by a spark (phase C, upper chart in Fig. 2).

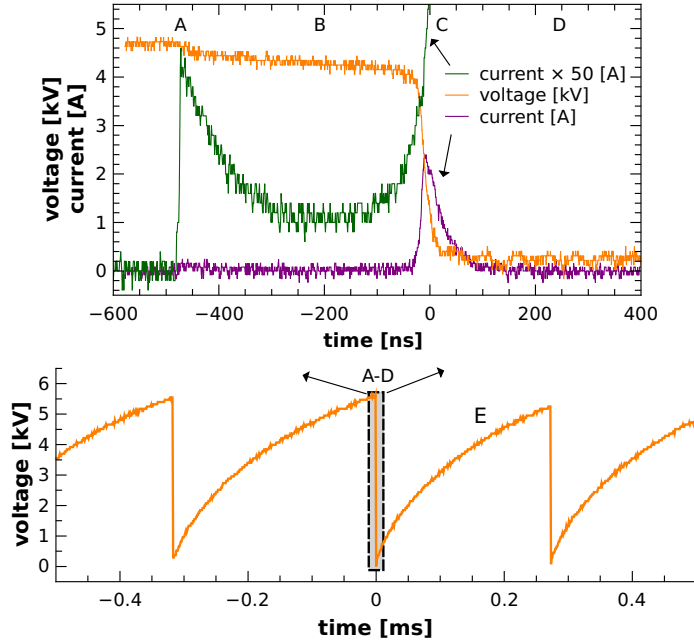


Figure 2: Typical voltage and current waveforms of Transient Spark, gap $d \approx 4.5$ mm, $C \approx 24$ pF, $R = 6.5$ M Ω , $f \approx 3.5$ kHz.

During the spark phase, the internal capacitor C discharges completely and the voltage V on the HV electrode drops to almost zero. The discharge current, given approximately by

$$I(t) \approx -C \times \frac{dV(t)}{dt}, \quad (1)$$

reaches a high value (~ 1 - 10 A) for a short time, and the n_e can exceed 10^{17} cm $^{-3}$ [10]. The gas temperature in the plasma channel shortly after the spark increases to at least 1500-3000 K [10]. However, the complete thermalization of plasma is not possible due to small amount of energy stored in C that is delivered to the gap during the spark phase.

Transition to an arc after the spark phase is restricted by the ballast resistor R . It limits the current delivered to the plasma by a DC power supply. As a result, the plasma starts to decay after the spark pulse (phase D, upper chart in Fig. 2). Eventually, the plasma resistance exceeds the R and the potential V on the stressed electrode gradually increases (phase E, lower chart in Fig. 2), as the capacitor C recharges. A new TS pulse, initiated by a new streamer, occurs when V reaches again the breakdown voltage V_{TS} . The TS is thus based on repetitive charging and discharging of C . The repetition frequency f of this process can be controlled by V_g approximately in the range 1-10 kHz [15].

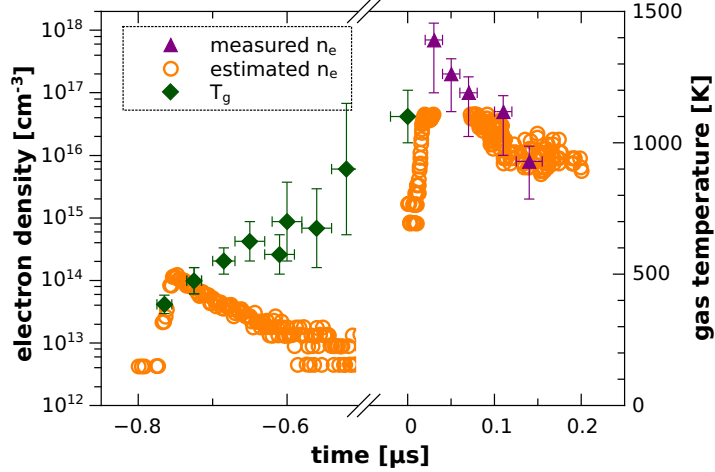


Figure 3: Evolution of temperature and electron density during TS discharge, $f \approx 2$ kHz and $C = 32 \pm 4$ pF.

The increase of f , achieved by increasing the generator voltage [15], is accompanied by changes of the several TS characteristics (decrease of the breakdown voltage, smaller and broader spark current pulses) and it also influences the breakdown mechanism. We observed significant shortening of the streamer-to-spark transition time τ [15, 16]. Above ~ 3 kHz, τ decreased from a few μ s down to ~ 100 ns. This is probably related to a 'memory' effect - gas pre-heating and accumulation of various species generated by previous TS pulses.

3 The Model Description

The density evolution of all species in a kinetic model can be derived from included reaction set:

$$\frac{dN_i}{dt} = S_i = \sum_{j=1}^{j=n} S_{ij}. \quad (2)$$

Here, S_i is a total production term for species X_i , while S_{ij} is a production term for species X_i in a specific reaction j . Next, n is the total number of reactions, and N_i is number density of species X_i . For the calculation of S_{ij} , the stoichiometric coefficients (lower case letters) of the X_i species in the j^{th} reaction



must be taken into the account:

$$S_{ij} = (a - a') * R_j. \quad (4)$$

The term R_j is the rate of the j^{th} chemical reaction:

$$R_j = k_j \times \prod_{m=i}^{m=i+l} N_m^{\alpha_m}, \quad (5)$$

where k_j is the reaction rate coefficient (rate constant), l is the total number of species involved in the j^{th} reaction, N_m is the actual density of m^{th} species, and α_m is the partial order of reaction with respect to the species m .

In praxis, it is necessary to solve this set of reactions numerically, using a solver of differential equations. We based our model on existing ZDPlasKin module [23] that includes a DVODE solver for numerical solution of system of ordinary differential equations. Authors of ZDPlasKin provide also a ready-to-use list of plasmachemical processes in nitrogen-oxygen mixtures, used also in Ref. [20], based mainly on Capitelli et al. [24]. We used this set of reactions (version 1.02 [25]) in our simulations too. It is a set of about 430 chemical reactions among 44 species, namely, molecules $\text{N}_2(\text{X}^1, v = 0 - 8)$, $\text{N}_2(\text{A}^3, \text{B}^3, \text{a}'^1, \text{C}^3)$, $\text{O}_2(\text{X}^3, v = 0 - 4)$, $\text{O}_2(\text{a}^1, \text{b}^1, 4.5\text{eV})$, O_3 , NO , atoms $\text{N}(\text{4S}, \text{2D}, \text{2P})$, $\text{O}(\text{3P}, \text{1D}, \text{1S})$, positive ions N^+ , N_2^+ , N_3^+ , N_4^+ , O^+ , O_2^+ , O_4^+ , NO^+ , O_2^+N_2 , negative ions O^- , O_2^- , O_3^- , O_4^- , NO^- and electrons. The electron impact excitation of other electronic states of nitrogen is also included, but the model assumes their instantaneous relaxation: $\text{N}_2(\text{W}^3, \text{B}'^3) \rightarrow \text{N}_2(\text{B}^3)$, $\text{N}_2(\text{a}^1, \text{w}^1) \rightarrow \text{N}_2(\text{a}'^1)$ and $\text{N}_2(\text{E}^3, \text{a}''^1) \rightarrow \text{N}_2(\text{C}^3)$. The generalized level $\text{O}_2(4.5\text{eV})$ corresponds to $\text{O}_2(\text{A}^3, \text{C}^3)$ and $\text{O}_2(\text{c}^1)$ states.

The rate constants of reactions between heavy species from this list are calculated from the thermodynamic gas temperature T_g . This temperature is frequently assumed to be equal for all ions and neutrals even in non-thermal plasma. This is no more true for electrons. Their energy is usually much higher, as well as their temperature (T_e). The rate constant for electron impact reactions must be calculated from electron energy distribution function (EEDF). The EEDF is usually obtained by solving Boltzmann equation for free electrons.

ZDplasKin package includes a Bolsig+ solver for the numerical solution of the Boltzmann equation. The principle and characteristic of Bolsig+ solver are described in more details in [26]. Set of required electron scattering cross sections was taken from the LXCat project database [27]. Namely, we used the databases of Phelps [28, 29] (N_2 , O_2 and NO) and Morgan [30, 31] ($\text{N}_2(\text{A}^3)$, $\text{O}_2(\text{a}^1)$, O_3 , O , and N). Besides the collisions with neutrals, the Bolsig+ solver also handles the electron-electron interactions if the degree of ionization exceeds 10^{-5} .

ZDPlasKin allows to use additional subroutines for more comprehensive control of simulation conditions, e.g. changes of the gas temperature, reduced electric field etc. Our major goal was to create a module compatible with ZDPlasKin with subroutines that would take into account fast changes of the reduced electric field strength E/N , gas temperature T_g and total density of neutrals N characteristic for the TS discharge. These profiles of E/N , T_g , and N resending the TS were constructed based on our experimental results and literature, as it is explained in the next sections.

4 Results and Discussion

The TS discharge, as described in section 2, can be divided to several phases. Each phase is characterized by different time scale and different dominant processes. In this work we focus on the relatively short ($< 1 \mu\text{s}$) active phase of the TS discharge, consisting of streamer, streamer-to-spark transition period and the spark phase. For the simplicity, we reflect this division also in this section and each TS phase is

described and discussed separately.

The active phase of the TS is characterized by a fast changes of E/N , T_g and T_e . It is therefore necessary to determine the density of many species that could influence the plasma induced chemistry with good temporal resolution (\sim ns), while processes such as diffusion can be neglected. We do not follow the changes of the gas composition during the relaxation phase of TS. Unlike in the short active phase of TS, we would have to include the diffusion processes and mixing with the ambient air. As a result, the presented model is more suitable for the TS at lowest frequencies, where effects resulting from the accumulation of species from previous pulses are weakest.

4.1 Streamer phase

Streamer is an ionization wave propagating the region with strong field from the high voltage electrode towards the grounded electrode. Streamer may lead to an electrical breakdown if it reaches the opposite electrode and creates a conductive plasma bridge between them. The streamer breakdown theory was introduced by Meek, Raether and Loeb [32–34] in the middle of the 20th century. However, because of the complexity of this problem, the study of the breakdown mechanism, streamers and their propagation still continues [35–44].

The modeling of streamer propagation requires at least 2D model using axi-symmetry assumption [45], though several studies using so called 1.5D symmetry exist [46]. The 0D kinetic model calculates densities of many species in a single point in space and obviously cannot be used to simulate propagation of the streamer. The influence of the streamer on the rates of chemical reactions in the 0D kinetic model can be introduced by using appropriate temporal evolution of E/N , based on streamer characteristics found in literature.

Although there are some differences in results from different streamer models [19, 37, 38, 43, 45], there are some common results that can be regarded as appropriate starting point. The upper limit for maximum n_e in streamer head is in order of 10^{14} cm^{-3} , which is in a good agreement with our experimental findings [10]. In the TS, the electron density in the plasma channel right after its establishment by the streamer is also in the order of 10^{14} cm^{-3} [10]. The maximum reduced field strength ($E/N_{max}^{str.}$) is usually not more than 250 – 270 Td in atmospheric air at 300 K, despite the fact that E/N as high as 600 Td in streamer head in dense media was reported [47]. After the head of the streamer, the field is much weaker. According to our estimate, the average reduced field established in the plasma after the streamer in TS is around 60-70 Td, assuming uniform axial distribution of the E/N [15].

We therefore decided to describe the E/N during the streamer by a function that would increase the electron density to 10^{14} cm^{-3} , with $E/N_{max}^{str.} = 270 \text{ Td}$, followed by decrease to $E/N_{bg} = 70 \text{ Td}$. For simplicity, we decided to use this value (70 Td) also for E/N before the streamer propagation. Finally, the time evolution of E/N in streamer phase of TS was simulated in our model by a function

$$E/N(t) = E/N_{bg} + \alpha \times \exp\left(\frac{-(t - t_s)^2}{2w^2}\right). \quad (6)$$

The t_s determines the center of the Gaussian peak representing streamer, with respect to the beginning of the simulation time. We usually used $t_s = 24 \text{ ns}$. The E/N_{bg} is the reduced field established in the

plasma after the streamer.

We performed set of calculations where we varied coefficient w , while the coefficient α was always adjusted to have $E/N_{max}^{str.} = 270$ Td in $t = t_s$. The goal was to obtain the maximum $n_e \approx 10^{14}$ cm $^{-3}$. For example, for the initial $n_e = 3 \times 10^8$ cm $^{-3}$, the initial composition of the gas 80% N_2 and 20% O_2 , $T_g = 300$ K and the pressure 1 atm, this was achieved for $w = 2.1$ ns (Fig. 4). Unless specified, we use this E/N profile (with $E/N_{max}^{str.} = 270$ Td, $w = 2.1$ ns, $E/N_{bg} = 70$ Td) as a starting point for the simulations presented in the next sections.

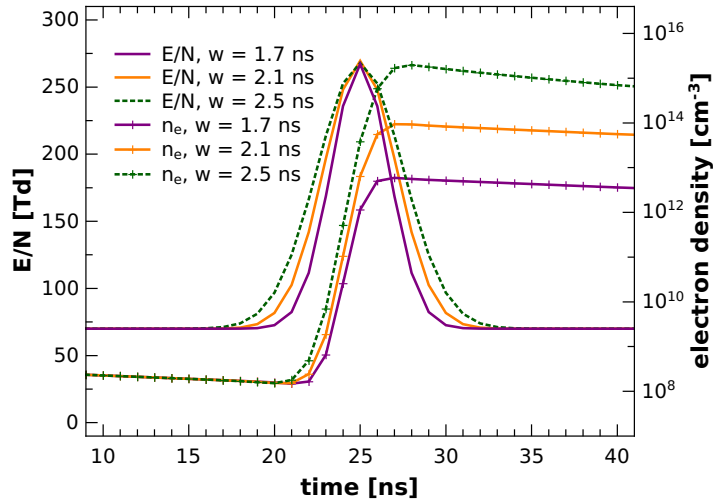


Figure 4: Evolution of electron density for different profiles of E/N simulating streamer.

4.2 Streamer-to-spark transition phase

The average E/N in the plasma channel after its establishment by the streamer, 60 – 70 Td, is too low to produce enough electrons by electron impact ionization reactions. Acceleration of the ionization processes certainly requires much stronger increase of E/N . In the TS, it can be achieved only by the significant decrease of N . The TS the breakdown mechanism postulated by Marode [48] based on the heating and hydrodynamic expansion of the plasma channel created by the streamer.

Actually, we experimentally observed that the streamer-to-spark transition in TS is probably governed by the heating of the gas inside the plasma channel up to ~ 1000 K [16]. However, besides the hydrodynamic expansion, the increase of T_g to 1000 K may also have direct effect on the gas phase chemistry [49]. The rate coefficients usually strongly depend on T_g . For example, the rate coefficients for the thermal detachment of electrons increase by four orders of magnitude between 300 and 1000 K [50]. We decided to verify the influence of T_g on the breakdown using our kinetic model.

We performed set of calculations where the E/N after the streamer remained constant (70 Td) for $1 \mu s$. The gas temperature was also constant, but it varied from 300 to 1000 K. The E/N during the streamer was simulated using eq. 6 with coefficient $w = 2.1$ ns. However, we had to decrease the coefficient α in order to achieve maximum electron density $\sim 10^{14}$ cm $^{-3}$, when we increased the T_g . Figure 5 shows the evolution of n_e from these calculations.

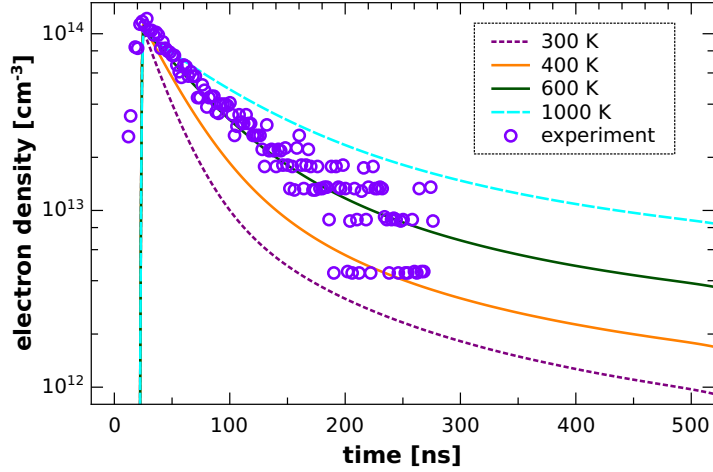
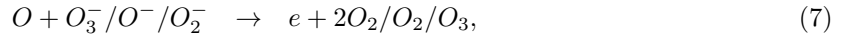


Figure 5: Evolution of electron density after the streamer for different gas constant temperatures.

These calculations show that the increase of the T_g up to 1000 K does not initiate the breakdown due to changes of rate coefficients of reactions. Although, the decrease of n_e after the streamer slows down with the increasing T_g . The increase of temperature up to 1000 K does not have very strong influence on the production of electrons after the streamer. The thermal detachment is not that significant as we expected. Even the direct electron impact ionization processes are more important, although the E/N is quite weak, 70 Td only (Fig. 6). The detachment of electrons from negative ions due to collisions with species such as O, $N_2(A^3\Sigma)$, or $O_2(a)$ is the most important. Here is the list of the most important reactions:



More significant is the influence of increasing T_g on the electron loss processes (Fig. 7). The most important reactions causing decrease of electron density at 300 K are:



Mainly reactions (11) and (12) depend strongly on T_g . At 600 K, the recombination of electrons with O_4^+ ions is already weak (Fig. 8), and in contrast to results presented in Ref. [41], it does not dominate even at 300 K. At 1000 K, the three-body attachment (eq. 11) slows down due to decrease of N , and the reaction (10) dominates completely.

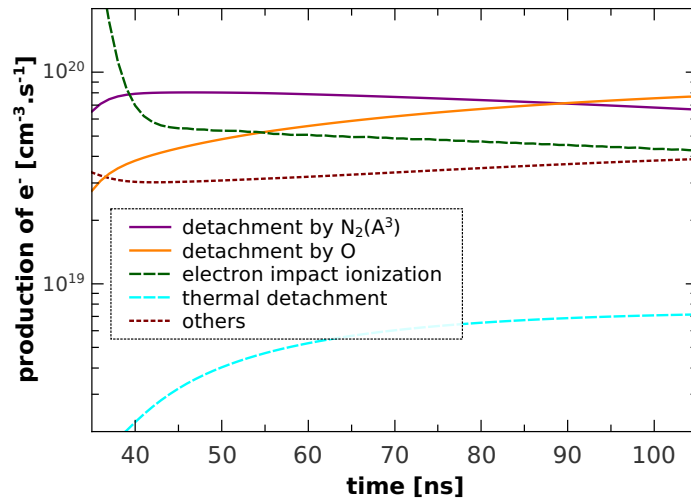


Figure 6: Major processes responsible for the production of electrons after the streamer, constant gas temperature and E/N , 1000 K and 70 Td, respectively.

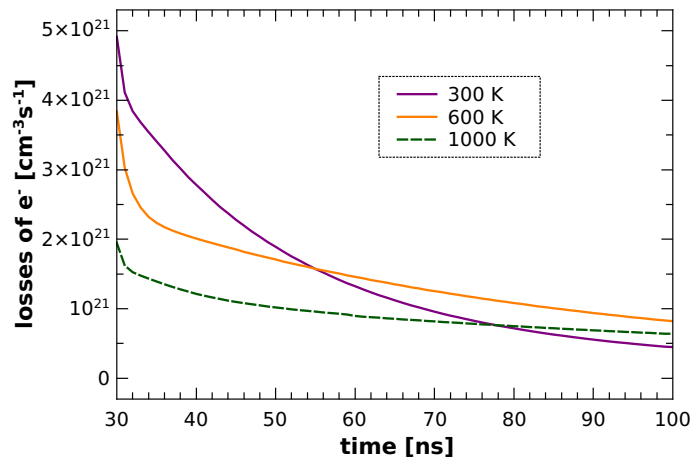


Figure 7: Electron losses after the streamer at different gas temperatures.

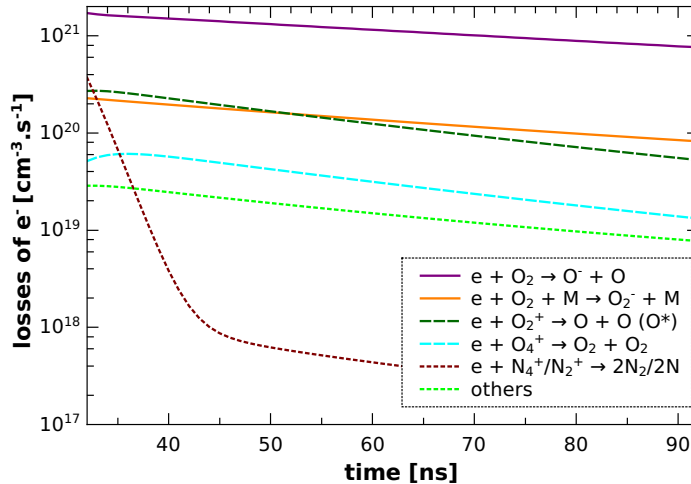


Figure 8: Major processes responsible for the losses of electrons after the streamer, constant gas temperature and E/N , 600 K and 70 Td, respectively.

The best agreement with experimental estimate of n_e was achieved for calculation with $T_g = 600$ K (Fig. 5). Based on the measured pre-heating of the gas inside the plasma channel at $f \approx 2$ kHz, we expected that the best agreement will be achieved for T_g between 300 K and 400 K. We therefore suppose that even in 'low' frequency TS regime ($f < 3$ kHz), a 'memory' effect due to accumulation of some species from previous TS pulses can play a certain role in the breakdown processes, causing slower decrease of n_e after the streamer.

Several species could influence the breakdown, for example metastable $O_2(a)$ species [36]. Based on the list of the most important electron production and loss processes (eq. 9 - 14), we suppose that the slower decrease of n_e after the streamer could be explained by accumulation of atomic oxygen species O. The accumulation of O species would accelerate the electron detachment from negative ions. Moreover, they are produced from molecular oxygen O_2 , and the decrease of the O_2 density would slow down the rate of electron attachment processes. The accumulation of O species in high concentration was experimentally observed in nanosecond repetitive pulsed discharge at 10 kHz [51].

We tried to simulate the influence of O species in our model by increasing initial density of O species (n_O) and decreasing initial density of O_2 . As we expected, the rate of n_e decrease after the streamer slowed down with the increasing n_O . However, the initial densities of other accumulated species could also influence the n_e evolution after the streamer. The current version of our model does not allow us to study this problem correctly, since we cannot perform calculation of sequence of pulses. These 'single pulse' calculations just show that the 'memory' effect related to changes of the gas composition by previous pulses have certain influence on the streamer-to-spark transition phase in the TS discharge.

This effect is certainly more important at higher f (≥ 4 kHz). It could explain almost direct transition from streamer to spark in TS at ~ 6 kHz [16], where a slow increase of current and n_e starts right after the streamer. However, the exponential increase of current and n_e characteristic for the initiation of the spark phase of TS requires another explanation. We suppose that it is necessary to accelerate also the electron impact ionization reactions. This can only be achieved by the increase of E/N , as discussed in

the next section.

4.3 Spark phase

In the TS, the increase of E/N after the streamer can be achieved only by the decrease of N . We therefore assume that the breakdown mechanism in TS is based on the gas density decrease suggested by Marode [48] and simulated by Naidis [52]. It can be summarized as follows: heating of the channel \rightarrow increase of the pressure \rightarrow hydrodynamic expansion \rightarrow decrease of N in the core of the channel \rightarrow increase of E/N \rightarrow acceleration of ionization processes. At higher frequencies, the breakdown is certainly influenced by species accumulated from the previous pulses, but the increase of E/N is probably crucial even at $f \geq 6$ kHz.

We are not able to calculate time evolution of gas density $N(t)$ with our 0D kinetic model. It is necessary to use at least 2D hydrodynamic model (assuming radial symmetry of discharge channel). For this reason, we tested the N profile (Fig. 9) from the simulations of Naidis [52]. Besides the hydrodynamic expansion, it handles also the radial diffusion of particles from the discharge channel. We suppose that this profile is the closest match to the TS discharge we found in the literature.

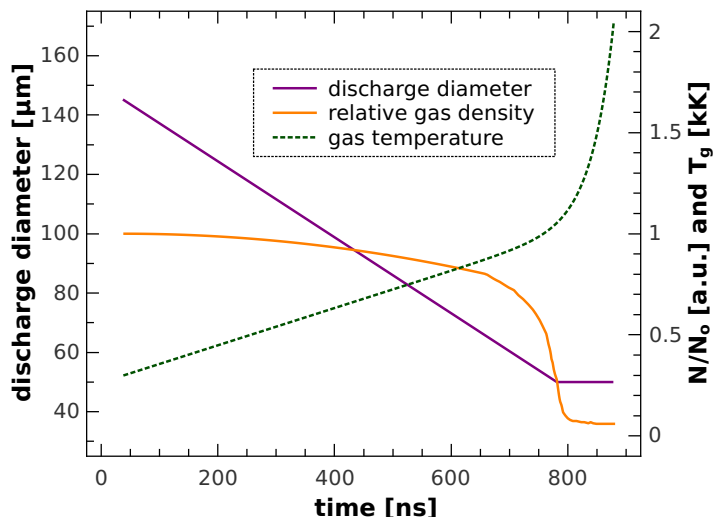


Figure 9: Input data for the simulation of the TS spark phase.

The changes of N according to the profile taken from Naidis starts in the calculation time 620 ns, so that the fastest rate of N decrease is reached in the moment when $T_g \approx 1000$ K. We extrapolated this profile and the N starts to decrease from $N_o = 2.5 \times 10^{19} \text{ cm}^{-3}$ right after the streamer, from the calculation time 40 ns. The rate of the extrapolated gas density decrease is proportional to the difference between the T_g and the ambient temperature (300 K). The T_g increases linearly during the streamer-to-spark transition phase from 300 K with the heating rate $9.2 \times 10^8 \text{ K.s}^{-1}$ according to the experimental findings (Fig. 3). From 1000 K, it starts to increase exponentially up to 2000 K (Fig. 9).

In order to calculate time evolution of reduced electric field strength E/N from the evolution of N , our model calculates time evolution of potential $V(t)$ between the electrodes (Fig. 10). We actually simulate the discharging of C via the plasma resistance R_p . The advantage of this approach is that

besides n_e , we calculate another variable that can be compared with experimental data - $V(t)$.

The decrease of potential ΔV^i for i -th calculation step can be expressed as

$$\Delta V^i = -V^{i-1} \frac{\Delta t}{C R_p^{i-1}}. \quad (15)$$

The R_p is related to the plasma conductivity σ_p by

$$R_p = \frac{4d}{\sigma_p \pi D_p^2}, \quad (16)$$

where d and D_p are the discharge channel length and the diameter, respectively. For approximation of D_p (Fig. 9), we used the FWHM of the spectrally unresolved radial intensity profile of the plasma channel after the Abel inversion [10]. At low TS repetition frequencies (below 4 kHz), we observed shrinking of the discharge channel diameter during the streamer-to-spark transition from $\sim 150 \pm 40 \mu\text{m}$ in the streamer phase, down to $\sim 50 \pm 20 \mu\text{m}$ in the spark phase. This behavior is in agreement with the calculations of Naidis [52].

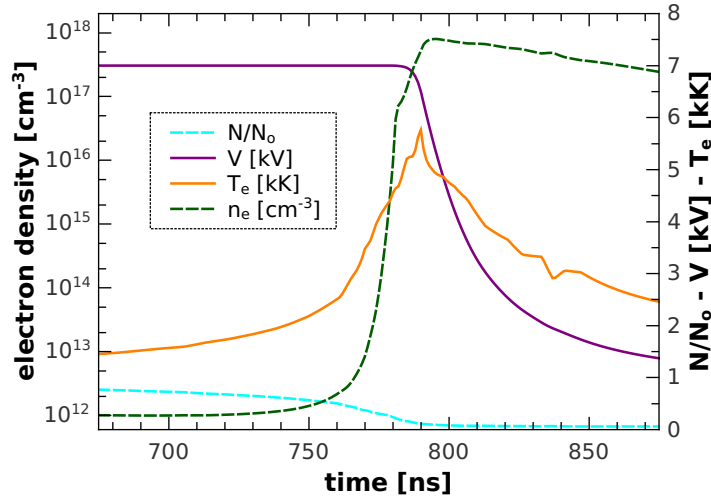


Figure 10: Calculated evolution of potential, electron density and temperature, $d=5$ mm, $C=30$ pF, initial potential 7 kV, discharge diameter evolution as shown on Fig. 9.

The plasma conductivity is calculated by the model from n_e :

$$\sigma_p = \frac{e^2 n_e}{m_e \nu_m}. \quad (17)$$

Here e and m_e are the electron charge and mass, respectively, and ν_m is the effective collision frequency of electrons with heavy particles, including ions. Finally, the $E/N(t)$ is derived from $V(t)$ and $N(t)$ assuming homogeneous axial potential distribution:

$$E/N(t) = cV(t)/N(t). \quad (18)$$

The constant c was chosen so that the evolution of E/N after the streamer starts from 70 Td.

The calculated E/N serves as input parameter for the Bolsig+ solver to calculate the electron energy distribution function, if the degree of ionization is below 10^{-3} . If the degree of ionization is higher,

the Bolsig+ solver is not suitable to calculate the EEDFs. In such a case, we use Maxwellian EEDFs defined by the electron temperature T_e , calculated from the E/N as if the plasma was weakly ionized. Besides this approximation, the weakest point of this approach is strong dependence of calculated plasma resistance on D_p . The uncertainty of experimentally measured plasma diameter is quite high. Moreover, the optical width of the discharge channel need not necessarily be identical with the "electrical" discharge diameter.

The decreases of D_p can cause temporal increase of R_p , even if the plasma conductivity increases. The minimum plasma diameter, $D_p = 50 \mu\text{m}$, causes that the R_p is still relatively high even during the TS spark phase. This can explain relatively slow decrease of calculated potential on Fig. 10, compared to measured voltage waveforms. As a result, the T_e decreases relatively slowly as well. Relatively high T_e means that ionization reactions generate electrons even during the "post-spark" phase (calculation time $>800 \text{ Td}$). This can explain slower decrease of calculated n_e compared to experimental data (Fig. 11).

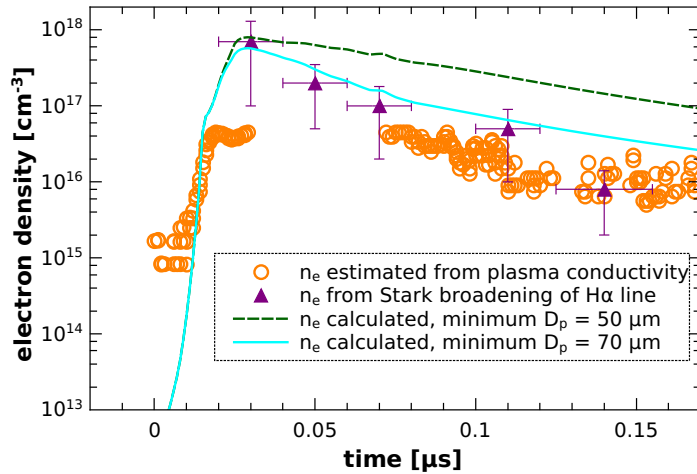


Figure 11: Comparison of calculated and measured electron densities during the spark phase of TS.

When we changed the minimum discharge diameter from 50 to 70 μm , we obtained better agreement between calculated and measured n_e . At least in case of n_e measured from the Stark broadening of the H_α line (Fig. 11). For D_p decreasing down to 70 μm , faster decrease of calculated potential, comparable with the measured waveforms, was also achieved. As a result, the T_e also decreased faster, down to $\sim 12000 \text{ K}$. This value is in a good agreement with the electron temperature derived from the Stark broadening of atomic lines after the TS spark current pulse ($\sim 10000 \text{ K}$) [10].

Further increase of minimum D_p in our calculations leads to even better agreement between measured and calculated TS characteristics (n_e , $V(t)$, T_e after the spark). However, we decided to present only data for minimum $D_p = 70 \mu\text{m}$, since it is still within the uncertainty of the experimentally observed D_p during the spark phase of TS ($50 \pm 20 \mu\text{m}$). Moreover, we could improve the match between experimental data and calculated electron density if we try to optimize value of C and initial potential $V(0)$.

Based on good agreement between measured and calculated electron density, we suppose that we can use the simulations with minimum $D_p = 70 \mu\text{m}$ to identify the most important electron production and

losses reactions during and after the TS spark phase. Naturally, the production of electrons dominates only during the initial part of the high current spark phase. Most electrons are produced by the electron impact ionization of N_2 (O_2) and N . Later, ~ 50 ns after the current peak, the production of electrons is maintained mostly by reactions between $N_2(a')$ and $N_2(A^3)$ species leading to generation of N_4^+ ions.

The electron loss processes dominate in the post-spark phase. During and right after the spark current pulse, the electrons are lost mostly due to recombination with N_2^+ ions (Fig. 12). In the later phase, the recombination with N^+ is very important. Recombination reactions with other ions, such as N_4^+ , NO^+ and O_2^+ are also not negligible. On the other hand, the electron attachment reactions are almost negligible. Mostly due to high gas temperature and low density of negative ions.

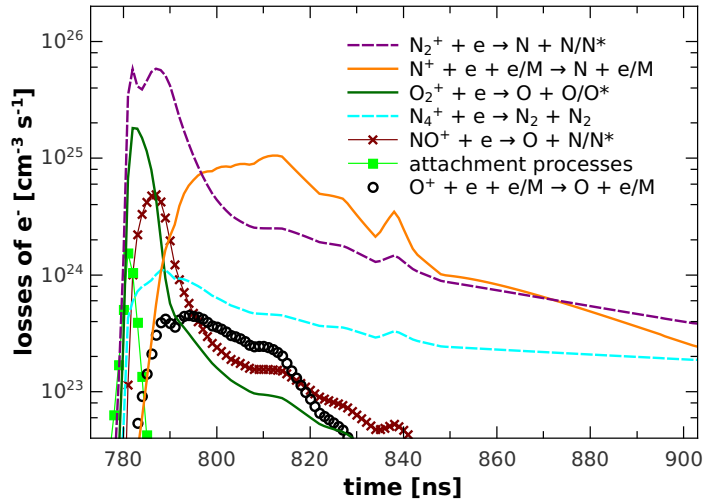


Figure 12: Major processes responsible for the losses of electrons during and after the TS spark phase.

5 Conclusions

Zero dimensional kinetic model based on ZDPlasKin simulating transient spark discharge was introduced in this work. Transient spark (TS) is a DC-driven self-pulsing streamer-to-spark transition discharge characterized by very short spark pulse duration (~ 10 - 100 ns). The electron density n_e as high as 10^{14} cm^{-3} in the streamer phase and 10^{17} cm^{-3} in the spark phase of the TS can be achieved. However, thanks to limited energy delivered to gap per pulse, the generated plasma stays out of equilibrium.

The goal of this work was to identify evolution of the reduced electric field E/N in different phases of TS (streamer, streamer-to-spark transition phase, spark) so that the calculated evolution of electron density n_e fits the experimental data. We focused on a single TS pulse in the current version of the model. In the further work we plan to extend the model to include the relaxation phase of the TS with much longer time scale (~ 100 μs - 1 ms), where the diffusion must be also taken into account. This will enable us to perform simulation of sequence of TS pulses.

Despite its limitations, the presented version of kinetic model enabled us to clarify the mechanism of the streamer-to-spark transition in TS. Previous experimental study indicated that breakdown in

TS occurs when the gas temperature inside the plasma channel created by the streamer increases to ~ 1000 K. Our calculations show that the breakdown is not directly related to the changes of plasma chemistry at 1000 K. This temperature is not high enough to accelerate the thermal detachment of electrons sufficiently. The heating of the gas inside the plasma channel leads to the local increase of the pressure, hydrodynamic expansion, decrease of the density of neutrals and thus increase of E/N . This accelerates the electron impact ionization processes crucial for the breakdown and spark formation. At ~ 1000 K, the pressure inside the channel probably reaches a critical value for the hydrodynamic expansion and shock wave formation.

This mechanism is valid for all TS repetition frequencies, though it can be influenced by a 'memory' effect at higher frequencies due to pre-heating and accumulation of various species created by previous TS pulses. Sensitivity analysis focused on major electron loss and production processes indicates the important role of the accumulated atomic oxygen species. They are produced from O_2 species. Lower density of O_2 means lower rate of electron attachment, while accumulated atomic oxygen species lead to acceleration of electron detachment processes. Further research of this memory effect using improved version of our kinetic model simulating sequence of pulses is needed to verify this hypothesis.

Acknowledgement

Effort sponsored by the Slovak Research and Development Agency APVV-0134-12, and Slovak grant agency VEGA 1/0918/15.

References

- [1] T. Kuwahara, T. Kuroki, K. Yoshida, N. Saeki, and M. Okubo. Development of sterilization device using air nonthermal plasma jet induced by atmospheric pressure corona discharge. *Thin Solid Films*, 523:2–5, 2014.
- [2] R. B. Gadri et al. Sterilization and plasma processing of room temperature surfaces with a one atmosphere uniform glow discharge plasma (OAUGDP). *Surf. Coat. Tech.*, 131:528–542, 2000.
- [3] H. Miao and G. Yun. The sterilization of escherichia coli by dielectric-barrier discharge plasma at atmospheric pressure. *Appl. Surf. Sci.*, 257:7065–7070, 2011.
- [4] V.E. Messerle, E.I. Karpenko, and A.B. Ustimenko. Plasma assisted power coal combustion in the furnace of utility boiler: Numerical modeling and full-scale test. *Fuel*, 126:294–300, 2014.
- [5] M. Cernak, J. Rahel, D. Kovacik, M. Simor, A. Brablec, and P. Slavicek. *Contrib. Plasma Phys.*, 44:492, 2004.
- [6] M. J. Gallagher, A. Gutsol, G. Friedman, and A. Fridman. Non-thermal plasma applications in air-sterilization. In *31st IEEE International Conference On Plasma Science*, Baltimore (Maryland), June 28- July 1 2004.

- [7] M. Sahni and B.R. Locke. Degradation of chemical warfare agent simulants using gas–liquid pulsed streamer discharges. *J. Hazard. Mater.*, B137:1025–1034, 2006.
- [8] I. Tanarro, V. J. Herrero, E. Carrasco, and M. Jiménez-Redondo. Cold plasma chemistry and diagnostics. *Vacuum*, 85:1120–1124, 2011.
- [9] M. Derakhshesh, J Abedi, and M Omidyeganeh. Modeling of hazardous air pollutant removal in the pulsed corona discharge. *Phys. Lett. A*, 373:1051–1057, 2009.
- [10] M. Janda, V. Martišoviš, L. Dvonč, K. Hensel, and Z. Machala. Measurement of the electron density in transient spark discharge. *Plasma Sources Sci. Technol.*, 23:Art. No. 065016 (12pp), 2014.
- [11] Z. Machala, M. Morvová, E. Marode, and I. Morva. Removal of cyclohexanone in transition electric discharges at atmospheric pressure. *J. Phys. D: Appl. Phys.*, 33:3198, 2000.
- [12] Z. Machala, M. Janda, K. Hensel, I. Jedlovský, L. Leštinská, V. Foltin, V. Martišoviš, and M. Morvová. Emission spectroscopy of atmospheric pressure plasmas for bio-medical and environmental applications. *J. Mol. Spectrosc.*, 243:194, 2007.
- [13] Z. Machala, I. Jedlovský, L. Chládeková, B. Pongráč, D. Giertl, M. Janda, L. Šikurová, and P. Polčic. Dc discharges in atmospheric air for bio-decontamination – spectroscopic methods for mechanism identification. *Eur. Phys. J. D*, 54:195, 2009.
- [14] Esther Hontanon, Jose Maria Palomares, Matthias Stein, Xiaoi Guo, Richard Engeln, Hermann Nirschl, and Frank Einar Krus. The transition from spark to arc discharge and its implications with respect to nanoparticle production. *J. Nanopart. Res.*, 15(9), SEP 2013.
- [15] M. Janda, V. Martišoviš, and Z. Machala. Transient spark: a dc-driven repetitively pulsed discharge and its control by electric circuit parameters. *Plasma Sources Sci. Technol.*, 20:Art. No. 035015 (10pp), 2011.
- [16] M. Janda, Z. Machala, A. Niklová, and V. Martišoviš. The streamer-to-spark transition in a transient spark: a dc-driven nanosecond-pulsed discharge in atmospheric air. *Plasma Sources Sci. Technol.*, 21:Art. No. 045006 (9pp), 2012.
- [17] T. Gerling, T. Hoder, R. Brandenburg, R. Bussiahn, and K.-D. Weltmann. Simulation of streamer-induced pulsed discharges in atmospheric-pressure air. *J. Phys. D: Appl. Phys.*, 46:Art. No. 145205, 2013.
- [18] T. Gerling, T. Hoder, R. Bussiahn, R. Brandenburg, and K.-D. Weltmann. Simulation of streamer-induced pulsed discharges in atmospheric-pressure air. *Plasma Sources Sci. Technol.*, 22:Art. No. 065012, 2013.
- [19] S. Kacem et al. Full multi grid method for electric field computation in point-to-plane streamer discharge in air at atmospheric pressure. *J. Comput. Phys.*, 231:251–261, 2012.

- [20] A. Flitti and S. Pancheshnyi. Gas heating in fast pulsed discharges in n₂-o₂ mixtures. *Eur. Phys. J. Appl. Phys.*, 45:21001, 2009.
- [21] J. Jeništa. Water-vortex stabilized electric arc: I. numerical model. *J. Phys. D: Appl. Phys.*, 32:2763–2776, 1999.
- [22] R. Barni et al. Chemical kinetics simulation of atmospheric pressure streamer in air. *J. Appl. Phys.*, 97:Art. No. 073301, 2005.
- [23] S. Pancheshnyi, B. Eismann, G.J.M. Hagelaar, and L.C. Pitchford. Computer code zdp_laskin. <http://www.zdpaskin.laplace.univ-tlse.fr> (University of Toulouse, LAPLACE, CNRS-UPS-INP, Toulouse, France), 2008.
- [24] M. Capitelli, C.M. Ferreira, B.F. Gordiets, and A.I. Osipov. *Plasma Kinetics in Atmospheric Gases*. Springer Series on Atomic, Optical, and Plasma Physics. Springer, 2000.
- [25] <http://www.zdpaskin.laplace.univ-tlse.fr/examples/04/>.
- [26] G.J.M. Hagelaar. Bolsig+: Electron boltzmann equation solver. <http://www.bolsig.laplace.univ-tlse.fr/how2use.php>, october 2013.
- [27] S. Pancheshnyi, S. Biagi, M.C. Bordage, G.J.M. Hagelaar, W.L. Morgan, and A.V. Phelps and L.C. Pitchford. The lxcat project: Electron scattering cross sections and swarm parameters for low temperature plasma modeling. *Chem. Phys.*, 398:148, 2012.
- [28] Phelps database. www.lxcat.net, retrieved on March 13, 2014.
- [29] A.V. Phelps and L.C. Pitchford. Anisotropic scattering of electrons by n₂ and its effect on electron-transport. *Phys. Rev. A*, 31:2932, 1985.
- [30] Morgan database. www.lxcat.net, retrieved on May 26, 2014.
- [31] www.kinema.com.
- [32] J.M. Meek. *Phys. Rev.*, 57:722–728, 1940.
- [33] H. Raether. *Electron Avalanches and Breakdown in Gases*. Butterworths, London, 1964.
- [34] L.B. Loeb. *Electrical Coronas*. University of California Press, Berkeley, 1965.
- [35] E. Marode. *J. Appl. Phys.*, 46:2005(I) and 2006(II), 1975.
- [36] J.J. Lowke. *J. Phys. D: Appl. Phys.*, 25:202, 1992.
- [37] R. Morrow and J. J. Lowke. Streamer propagation in air. *J. Phys. D: Appl. Phys.*, 30:617–627, 1997.
- [38] A.A. Kulikovskiy. *IEEE Trans. Plasma Sci.*, 26:1339–1346, 1998.
- [39] A. Larsson. *J. Phys. D: Appl. Phys.*, 31:1100–1108, 1998.

- [40] G.V. Naidis. *J. Phys. D: Appl. Phys.*, 32:2649–2654, 1999.
- [41] N.L. Aleksandrov and E.M. Bazelyan. *Plasma Sources Sci. Technol.*, 8:285–294, 1999.
- [42] A.A. Kulikovskiy. *IEEE Trans. Plasma Sci.*, 29:313–317, 2001.
- [43] A. Bourdon, Z. Bonaventura, and S Celestin. Influence of the pre-ionization background and simulation of the optical emission of a streamer discharge in preheated air at atmospheric pressure between two point electrodes. *Plasma Sources Sci. Technol.*, 19:Art. No. 034012 (10pp), 2010.
- [44] J. Jansky et al. *J. Phys. D: Appl. Phys.*, 44:Art. No. 335201, 2011.
- [45] A. A. Kulikovskiy. Positive streamer between parallel plate electrodes in atmospheric pressure air. *J. Phys. D: Appl. Phys.*, 30:441– 450, 1997.
- [46] P. Bayble and B. Cornebois. Propagation of ionizing electron shock waves in electrical breakdown. *Phys Rew A*, 31:1046, 1985.
- [47] N.Yu. Babaeva and G.V. Naidis. On streamer dynamics in dense media. *J. Electrostat.*, 53:123–133, 2001.
- [48] E. Marode, F. Bastien, and M. Bakker. *J. Appl. Phys.*, 50:141–146, 1979.
- [49] E. Marode, D. Djermoune, P. Dessante, C. Deniset, P. Segur, F. Bastien, A. Bourdon, and C. Laux. *Plasma Phys. Control. Fusion*, 51:124002, 2009.
- [50] S.I. Kozlov, V.A. Vlaskov, and N.V. Smirnova. *Space Res. (in Russian)*, 26:738, 1988.
- [51] G.D. Stancu, F. Kaddouri, D.A. Lacoste, and C.O. Laux. Atmospheric pressure plasma diagnostics by oes, crds and talif. *J. Phys. D: Appl. Phys.*, 43:124002, 2010.
- [52] Naidis G. Simulation of streamer-induced pulsed discharges in atmospheric-pressure air. *Eur. Phys. J. Appl. Phys.*, 47:Art. No. 22803, 2009.